PROCEEDINGS OF SPIE

SPIEDigitalLibrary.org/conference-proceedings-of-spie

Development of precision Wolter mirrors for solar x-ray observations

Taro Sakao
Satoshi Matsuyama
Takumi Goto
Jumpei Yamada
Shuhei Yasuda
Kazuto Yamauchi
Yoshiki Kohmura
Ayumi Kime
Akira Miyake
Tadakazu Maezawa
Hirokazu Hashizume
Yoshinori Suematsu
Noriyuki Narukage
Shin-nosuke Ishikawa

SPIE.

Development of precision Wolter mirrors for solar x-ray observations

Taro Sakao*[a,h], Satoshi Matsuyama[b], Takumi Goto[b], Jumpei Yamada[b], Shuhei Yasuda[b], Kazuto Yamauchi[b], Yoshiki Kohmura[c], Ayumi Kime[d], Akira Miyake[e], Tadakazu Maezawa[f], Hirokazu Hashizume[f], Yoshinori Suematsu[g], Noriyuki Narukage[g], and Shin-nosuke Ishikawa[a]

[a]Institute of Space and Astronautical Science, Japan Aerospace Exploration Agency, 3-1-1 Yoshinodai, Chuo-ku, Sagamihara, Kanagawa 252-5210, Japan

[b]Department of Precision Science and Technology, Graduate School of Engineering, Osaka University, 2-1 Yamada-oka, Suita, Osaka 565-0871, Japan

[c]SPring-8/RIKEN, 1-1-1 Kouto, Sayo-cho, Sayo-gun, Hyogo 679-5148, Japan

[d]Space Tracking and Communications Center, Japan Aerospace Exploration Agency, 2-1-1 Sengen, Tsukuba, Ibaraki 305-8505, Japan

[e]Canon Inc., 20-2 Kiyohara-Kogyodanchi, Utsunomiya, Tochigi 321-3292, Japan

[f]Natsume Optical Corp., 1200-29 Kawaji, Iida, Nagano 399-2431, Japan

[g]National Astronomical Observatory of Japan, 2-21-1 Osawa, Mitaka, Tokyo 181-8588, Japan

[h]Department of Space and Astronautical Science, School of Physical Sciences, The Graduate University for Advanced Studies (SOKENDAI), 3-1-1 Yoshinodai, Chuo-ku, Sagamihara, Kanagawa 252-5210, Japan

ABSTRACT

High resolution imagery of the Sun's X-ray corona provides an essential clue in understanding dynamics and heating processes of plasma particles there. However, X-ray imagery of the Sun with sub-arcsecond resolution has so far never been conducted due to severe technical difficulty in fabricating precision Wolter mirrors. For future X-ray observations of the solar corona, we are attempting to realize precision Wolter mirrors with sub-arcsecond resolution by adopting advanced surface polish and metrology methods to sector mirrors which consist of a portion of an entire annulus, by direct polishing onto the mirror substrate.

Based on the knowledge obtained through fabrication of the first (in 2013) and second (in 2014) engineering Wolter mirrors and subsequent evaluations on their X-ray focusing performance, the third engineering mirror was made in 2015−2016. The primary target of improvement over the second mirror was to suppress figure error amplitude especially for spatial frequencies around 1 mm^{-1} and to suppress the large astigmatism that was present in the second mirror, by introducing improved deterministic polish and smoothing on the precision mirror surfaces (32.5 mm × 10 mm in area for both parabola and hyperbola segments), as well as by careful characterization of the systematic error in the figure measurement system for the precision polish. Measurements on the focusing performance of thus-fabricated third Wolter mirror at SPring-8 synchrotron facility with 8 keV X-rays demonstrated that the mirror attained sub-arcsecond focusing performance with its HPD (half-power diameter) size reaching as small as ~0.2 arcsec for meridional focusing while ~0.1 arcsec for sagittal focusing. The meridional focusing achieved nearly diffraction limited performance (~0.12 arcsec FWHM for the PSF core). We also confirmed that the large astigmatism noted in the second mirror was correctly removed in the third mirror with the correction of the above-mentioned systematic error.

Keywords: Wolter mirror, X-ray telescope, solar corona, sub-arcsecond imagery, synchrotron X-rays, coherent X-rays

*sakao@solar.isas.jaxa.jp; www.isas.jaxa.jp/e/, www.isas.jaxa.jp/sokendai/e

Advances in X-Ray/EUV Optics and Components XII, edited by Christian Morawe, Ali M. Khounsary, Shunji Goto, Proc. of SPIE Vol. 10386, 103860E · © 2017 SPIE
CCC code: 0277-786X/17/$18 · doi: 10.1117/12.2273507

1. INTRODUCTION

It has been revealed with X-ray observations from space, particularly with *Yohkoh*[1] and *Hinode*[2] solar observatories, that the solar corona whose temperature reaching beyond 1 MK shows a wide variety of active phenomena including large-scale re-structuring of the magnetic field[3], creation of super-hot (exceeding ~30 MK) plasmas and acceleration of particles during flares[4, 5], and even gigantic mass ejections known as coronal mass ejections (CMEs) towards the interplanetary space[6]. Recent observations in EUV wavelengths from space have suggested that there are sub-arcsecond structures in the corona present and that such fine structures are responsible for supplying hot materials upward into the corona[7] thus would be relevant to the heating of the corona[8]. Some of the fine structures could reflect magnetic structure of the corona in the form of braided magnetic field lines[9]. Thus it has become widely perceived that resolving fine structures in the corona is essential in understanding dynamics and heating of the coronal plasmas.

As soft X-rays (with energy range from ≲1 keV to ~10 keV) can efficiently trace energized electrons in the corona, they are particularly suited for observing high energy processes (such as creation of high temperature plasmas well beyond 20 MK and acceleration of plasma electrons) and their relationship with the associated magnetic structures in the corona. However, sub-arcsecond imagery in the soft X-ray range with Wolter I optics[10] has so far remained extremely difficult due to severe requirements on the surface figure of the mirror[11], demanding years of polish hence resulting in huge amount of cost. As a result, sub-arcsecond imagery for astrophysical applications has so far only been accomplished by the *Chandra* X-ray observatory[12], but has never been made for the Sun.

With recent advances in precise surface metrology and precision polish, we have been attempting to realize sub-arcsecond (in terms of half-power diameter; HPD) Wolter I mirrors for future solar observations, by means of direct polishing onto glass substrates[13, 14, 15, 16]. We employ sector mirrors consisting of a part of an entire annulus, which enable access of metrology and precision polish equipments to the mirror surface much easier than that with an annular shape. In section 2, target specification of Wolter mirrors for future solar observations is summarized. In section 3, we present key issues identified through the measurements on the X-ray focusing performance of the second engineering mirror[17] (precision-polished in 2014) that was made following the first attempt in 2013[16], as well as design parameters for the second and third engineering mirrors. In section 4, we describe polishing approach adopted for the third mirror (fabricated in 2015−2016) as well as the result of the measurements on its X-ray focusing performance, followed by summary in section 5.

2. TARGET SPECIFICATION OF WOLTER MIRRORS FOR FUTURE SOLAR OBSERVATIONS

Scientific objectives to be addressed with sub-arcsecond imagery of the soft X-ray solar corona, in particular those coupled with photon-counting capability for the focal-plane detector, are discussed in Sakao et al. 2013[15] together with target specification for the Wolter mirrors. In addition to high spatial resolution imaging performance to resolve fine structures of hot plasmas in the corona, combination with photon-counting (imaging-spectroscopy) capability covering up to ~10 keV is particularly powerful in investigating magneto-hydrodynamic (MHD) structures in flares, such as possible fast/slow shocks, and could even address generation process(es) of supra-thermal electrons out of thermal plasmas in the corona that will eventually emit hard X-rays as they are accelerated. Table 1 summarizes target specification of precision Wolter I mirrors for future observations of the Sun. Towards this goal, a series of engineering mirrors have been developed.

Table 1. Target specification of precision X-ray Wolter I mirrors for future observations of the solar corona.

Item	Description	Note
Energy range	~0.5 − ~10 keV	
Angular resolution	< 1 arcsec HPD	Defined at 2 and 8 keV
Off-axis scattering	$\lesssim 10^{-5}$ of the PSF peak at 1-arcmin off-axis position	Defined at 8 keV
Geometric area	~0.5 − 1.5 cm^2 (TBD)	

3. ENGINEERING MIRROR #2

3.1 Design Parameters for the Engineering Mirror

Following fabrication and subsequent measurement in X-rays of the first engineering Wolter I mirror (Engineering Mirror #1; Sakao et al. 2014[16]), the second engineering Wolter I mirror (Engineering Mirror #2) was fabricated. Unlike Engineering Mirror #1 for which only a deterministic polishing method (MRF; Magnetorheological Finishing[18]) was employed, the precision polish for the Engineering Mirror #2 was made by a combination of MRF and smoothing while metrology of the surface figure performed by combining mechanical and optical/interferometric measurements with spatial-scale-dependent filters applied to the metrology results to take into account efficiency and long-term trend of each measurement method. Table 2 summarizes design parameters for the Engineering Mirror #2. These parameters are mostly originated from a possible future solar X-ray telescope discussed in previous literatures[13, 14, 15, 16]. The same design parameters were adopted for Engineering Mirror #3 which will be described in the subsequent section.

Table 2. Design parameters for the Engineering Mirror #2 and #3.

Item	Description	Note
Substrate	CLEARCERAM-Z HS	
Focal length	4000 mm	
Plate scale	1" / 20 μm	
Surface figure profile	Pure Wolter I	
Grazing-incidence angle	0.45 deg.	Angle at the parabola-hyperbola intersection
Mirror reflection area	32.5 mm × 10 mm for both parabola and hyperbola sections	(Along the optical axis direction) × (Along the cylindrical direction)
Arc radius	125.7 mm	Radius of curvature of the mirror surface along the cylindrical direction
Arc angle	4.6 deg.	Angle sustained by the mirror width (along the cylindrical direction) from the optical axis
Coating	Pt 100 nm + Cr 10 nm for binding layer	Coated by vapor deposition

3.2 Focusing Performance of the Engineering Mirror #2

The Engineering Mirror #2 was put to X-ray measurements in February 2015 at BL29XUL beam line[19] of SPring-8 synchrotron facility. The measurements were made with 8 keV X-rays. The experiment hatch used for the measurements is located away by 1 km from the synchrotron storage ring, providing highly parallel beam of X-rays. Furthermore, this beam line is designed to provide X-rays of high spatial coherence thus wave-optical calculations can be applied in interpreting and predicting focused beam profiles from surface figure profiles of mirrors. Details of the measurement setup is given in Sakao et al. 2015[17].

The X-ray measurements on the Engineering Mirror #2 provided the following findings.

1. The FWHM size of the PSF core reached as small as 4 μm, corresponding to an angular scale of 0.2", at each of the sagittal and meridional best on-axis focus positions.
2. The HPD size of the focus profile remained at ~3" (~60 μm) due to a large amount of small-angle scatter just outside the PSF core.
3. There was significant astigmatism present between the sagittal and meridional focusing in which the best meridional focus position was shifted towards the mirror by ~10% (~40 cm) of the designed focal length.
4. The large-angle scattering profiles of the mirror indicate that the scattering level at 1-arcmin off-axis position was well below 10^{-4} of the PSF peak.

Items 2 and 3 were identified as the major issues needed to be improved for realizing precision Wolter mirrors.

4. ENGINEERING MIRROR #3

4.1 Precision Polish for the Engineering Mirror #3

The third engineering Wolter I mirror (Engineering Mirror #3) was fabricated so as to improve, to the best of fabrication capability, the issues identified in the Engineering Mirror #2. Figure 1 shows the PSD profiles of the surface figure errors for the Engineering Mirror #2 (data points in colors) in comparison with those of the Engineering Mirror #1 (data points in gray). The profiles were generated by combining both mechanical as well as optical/interferometric measurements for each of the parabola and hyperbola segments with spatial-frequency-dependent PSD values defined as follows:

$$\mathrm{PSD}(f) = \frac{1}{L}\left|\int_0^L e^{2\pi i f x} E(x)\,dx\right|^2 ,$$

where f is the spatial frequency, $E(x)$ is the surface figure error at the location x on the mirror, and L is the extent of the mirror surface[11]. For readers' reference, integrating the above PSD(f) over a spatial frequency range [$f_{\min}$, $f_{\max}$] gives the surface roughness σ for the corresponding spatial frequency range[11]:

$$\sigma = \sqrt{\int_{f_{\min}}^{f_{\max}} \mathrm{PSD}(f)\,df} .$$

Through wave-optical calculations we have identified that the large amount of small-angle scatter seen in the Engineering Mirror #2 (Item 2 in section 3.2) was due to ripples in the figure present in around ~1 mm^{-1} spatial frequency range, and that if we were successful in reducing amplitudes of the surface figure errors by a factor of 2 in the 0.3−3 mm^{-1} range, we would expect sub-arcsecond HPD size for the focus profiles. The improvement of the figure error amplitudes in this spatial frequency range was thus set as our next target for the precision polish (Figure 1).

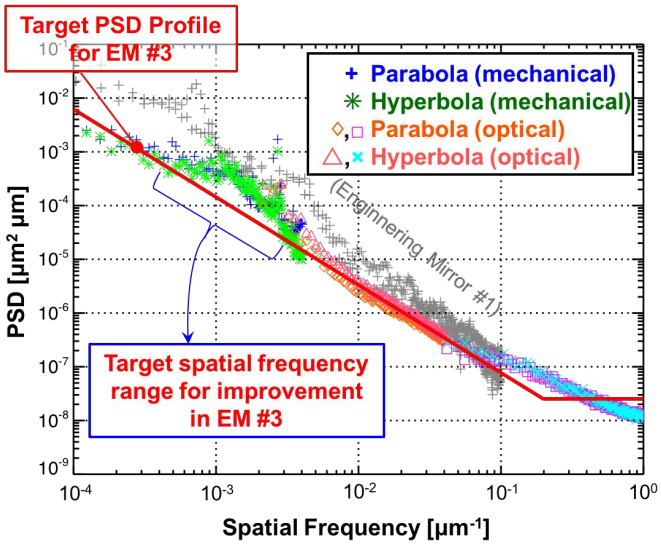

Figure 1. PSD profiles of surface figure errors for the Engineering Mirror #2 (data points in colors). Those for the Engineering Mirror #1 are shown in gray for comparison. Not much improvement was made in the spatial frequency range around 1 mm^{-1} which resulted in enhanced small-angle scatter just outside the PSF core in the Engineering Mirror #2. The target PSD profile for the Engineering Mirror #3 is shown in red lines that chiefly aimed at the improvement of the PSF profile in the above-mentioned spatial frequency range.

Another major issue with the Engineering Mirror #2 was that there was large astigmatism present between sagittal and meridional focusing (Item 3 in section 3.2). The deviation in focal length for meridional focusing corresponds to an incorrect radius of curvature in the meridional direction introduced by an error in sag of 6.5 nm in the mirror area (whose

spatial extent was 32.5 mm). After careful review of the figure measurement system employed during the precision polish, we have identified that a systematic error in the mechanical measurement system had introduced the sag error during the polish of the Engineering Mirror #2 (Figure 2), thus caused the notable astigmatism in the meridional direction of the mirror.

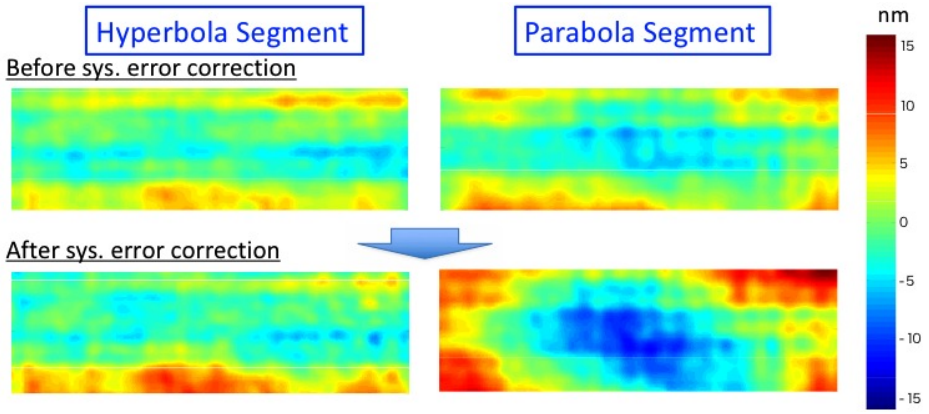

Figure 2. Comparison of the mechanical measurement results for the surface figure errors before and after correcting the systematic error in the mechanical measurement system. Design profiles and tilt components were subtracted from each of the metrology results. After the correction of the systematic error (bottom row), the average of the parabola (second-order polynomial) coefficients for the parabola and hyperbola segments turned out to be 2.75×10^{-8} mm^{-1}, which was in good agreement with that estimated from the observed astigmatism in X-rays (2.71×10^{-8} mm^{-1}) for the Engineering Mirror #2.

The Engineering Mirror #3 was fabricated using the same mirror substrate and the polishing area as those for the Engineering Mirror #2. Similar to the Engineering Mirror #2, the precision polish of the Engineering Mirror #3 was conducted by a combination of deterministic polish (MRF) and smoothing, with metrology of the surface figure performed with the same spatial-frequency filters applied to the metrology results from mechanical and optical/ interferometric measurements.

We identified that, through fabrication and subsequent X-ray measurement of the Engineering Mirror #2, the figure error correction around the spatial frequency of 1 mm^{-1} was crucial for achieving sub-arcsecond HPD. Hence we adopted a smaller polishing head for MRF than that used for the Engineering Mirror #2 with which we aimed to perform deterministic polish in spatial scales down to as small as ~0.5 mm as discussed in Sakao et al. 2015[17]. However, it turned out that the MRF polish, in combination with the filtered figure measurement data based on which the MRF polish was to be performed, would not be much effective for spatial scales below ~2−1 mm while there was a risk of introducing unwanted scratch features (though did not severely affect imaging performance) on the mirror surface to be generated by the polish. Thus, after the completion of the MRF polish that corrected the figure error down to ~2−1 mm (which was made after smoothing), we decided not to perform the next MRF polish which originally aimed to perform figure error correction in the spatial scale from ~2−1 mm down to ~0.5 mm range. Figure 3 depicts the final PSD profiles of the figure errors for parabola and hyperbola mirror segments of the Engineering Mirror #3. The profiles were generated by combining both mechanical and optical/interferometric metrology measurements. In the figure, the target PSD profile for the Engineering Mirror #3 is shown by a solid pink line while the dashed pink line illustrates approximately the as-built PSD profile for the Engineering Mirror #1. The PSD profile for the *Chandra* mirror[11, 12] is also shown in orange for comparison. Since we decided not to perform the deterministic MRF polish for the spatial scales below ~2−1 mm while smoothing could cover the spatial scales up to ~1−2 mm, we see there still exists slight excess in the figure error PSD over the target PSD profile in the spatial range from ~1 mm to ~2 mm (~5×10^{-4} μm^{-1} to ~1×10^{-3} μm^{-1} in spatial frequencies in Figure 3). However, we confirmed, through wave-optical evaluation utilizing the metrology data, that the mirror would have good imaging performance of sub-arcsecond HPD (and also FWHM size of the focusing core) in X-rays which was the basis of our decision of skipping the final MRF polish.

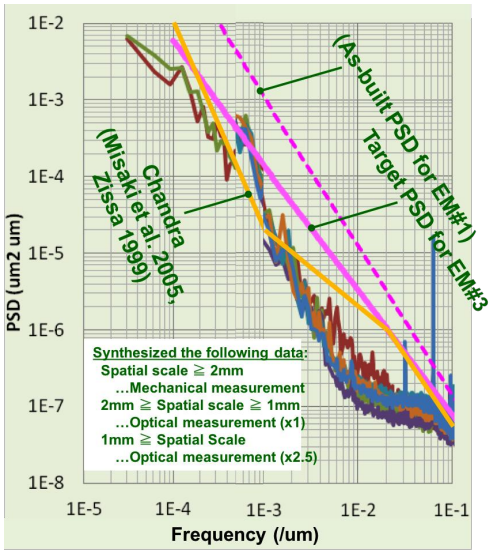

Figure 3. PSD profiles of surface figure errors of the Engineering Mirror #3 measured after the precision polish was completed. Measurement results on the parabola and hyperbola segments are overlaid in the figure.

After the precision polish was completed, the mirror was coated with platinum (Pt) by vapor deposition with chromium (Cr) being the binding layer to the mirror substrate (Table 2). For future development of precision Wolter mirrors, we plan to employ sputtering deposition with coating material whose atomic number larger than Pt (such as iridium (Ir)) to increase the energy range of total reflection for X-rays towards higher energies. Figure 4 shows the Engineering Mirror #3 after completing the coating with Pt. The precision polish was made for an area of 32.5 mm (along the optical axis direction) × 10 mm (along the cylindrical direction) on the mirror substrate, for each of the parabola and hyperbola segments. The coating was made only to the precision polish areas to avoid unwanted X-rays on the focal plane reflected on the mirror surfaces with poor surface figure quality. Two of the sides of the mirror substrate were finished to serve as reference surfaces that represented the mirror optical axes with respect to the incident X-ray beam.

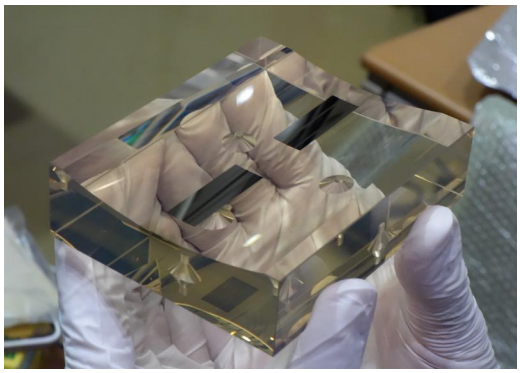

Figure 4. The Engineering Mirror #3 after Pt coating (seen in gray on the mirror substrate) on the precision Wolter surfaces. The mirror area in front is the parabola segment whereas that to the rear hyperbola segment.

4.2 Focusing Performance Measurements of the Engineering Mirror #3

Measurements on the X-ray focusing performance of the Engineering Mirror #3 was performed at SPring-8 BL29XUL beam line in December 2016, with the same experiment hatch (EH4) as the measurements for previous engineering mirrors. Figure 5 presents experiment apparatus for the X-ray characterization measurements on the Engineering Mirror

#3. The mirror was placed near the injection port of synchrotron X-rays to the hatch, on a precision 6-axes stage (hexapod; Figure 5 *left*) with which the injection angle of the X-rays to the mirror was adjusted. The mirror surface was set to be mostly in the horizontal plane. The area of the mirror (parabola section of the Wolter mirror) illuminated with X-rays was adjusted by a pair of horizontal and vertical slits placed in between the injection port and the mirror. X-rays then went through an ion chamber which was used for normalizing X-ray intensity. For the measurements, 8 keV X-rays were used. The right panel of Figure 5 shows the overall view of the experiment setup in EH4. A CMOS image sensor with a scintillator was placed in the focal plane (4 m away from the mirror) when taking two-dimensional intensity distribution of the focused X-rays while it was replaced by a PIN photo-diode when measuring detailed X-ray focus profiles with wire/knife-edge scans. A vacuum pipe, sealed with a 75 μm-thick polyimide film on each end, was placed in between the mirror and the focal plane to minimize attenuation of the 8-keV X-rays with air. The measurement setup was almost identical to those for the Engineering Mirror #2[17].

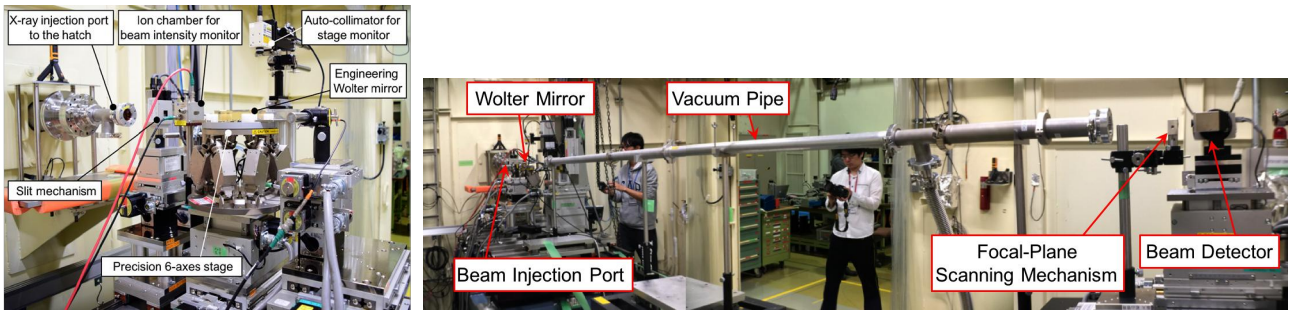

Figure 5. Experiment apparatus for the X-ray characterization measurements on the Engineering Mirror #3, at SPring-8 BL29XUL/EH4. *Left:* Measurement configuration around the mirror. X-rays are injected from the left side of the panel (shown as "X-ray injection port to the hatch") pass through the slit mechanism (to adjust the beam size) and the ionization chamber (to monitor beam intensity) and are reflected on the surfaces of the Wolter mirror and proceed towards the focal-plane. *Right:* Overview of the experiment setup, including the measurement setup around the mirror (left side of the panel) and the focal-plane detector (right side). A vacuum pipe was prepared along the path of the X-rays towards the focal plane.

Figure 6 presents intensity distribution, in logarithmic scale, of 8 keV X-rays focused with the Engineering Mirror #3, obtained with the CMOS image sensor. In the figure, meridional direction of the mirror is shown horizontally (upward direction in the experiment setup corresponds to the leftward in the figure). It is noted there are several intensity enhancements along the meridional direction. These features are caused by periodic ripples in the meridional direction in both the parabola and hyperbola segments of the mirror generated in association with the smoothing method applied for the precision polish. The presence of the ripples are recognized as spikes seen in the 10^{-2} to 10^{-1} μm^{-1} spatial frequency range in Figure 3. While the relative X-ray intensity of these features are several orders of magnitude smaller than the focusing core, further improvement in the smoothing to suppress the generation of these ripples is now under way.

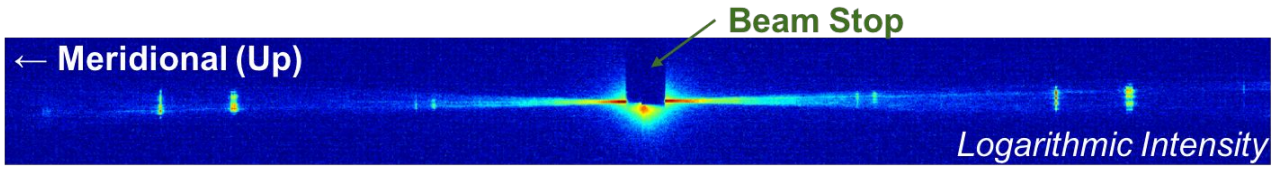

Figure 6. Intensity distribution of the focused X-rays in logarithmic scale, measured with the two-dimensional CMOS image sensor with a scintillator of Ce:YAG ceramics (100 μm in thickness) attached in front of it. In order to avoid X-rays scatter inside the scintillator, a beam stop was inserted to prevent the core portion of the focusing X-rays to illuminate the image sensor.

Figure 7 shows large-angle scattering profiles at the focal plane for the meridional (top panel) and sagittal (bottom panel) directions of the Engineering Mirror #3. The profiles were obtained by wire/knife-edge scans with the PIN photo-diode. The entire precision-polished mirror area was illuminated with X-rays. The mirror attained the targeted scattering performance of $\lesssim 10^{-5}$ of the PSF peak at 1-arcmin off-axis position (Table 1). Moreover, the scattering level at 10-arcsec off-axis position was as low as well below 10^{-3} of the PSF peak, reaching as close as 10^{-4}. This low-scattering performance of the mirror would provide crucial benefit in observing dark features in the X-ray solar corona that are expected to reflect key MHD processes for energizing solar flares (e.g., magnetic reconnection), without being obscured by scattered X-rays from nearby bright X-ray sources created as by-products of magnetic energy release (such as those created by chromospheric evaporation) during the course of the flare.

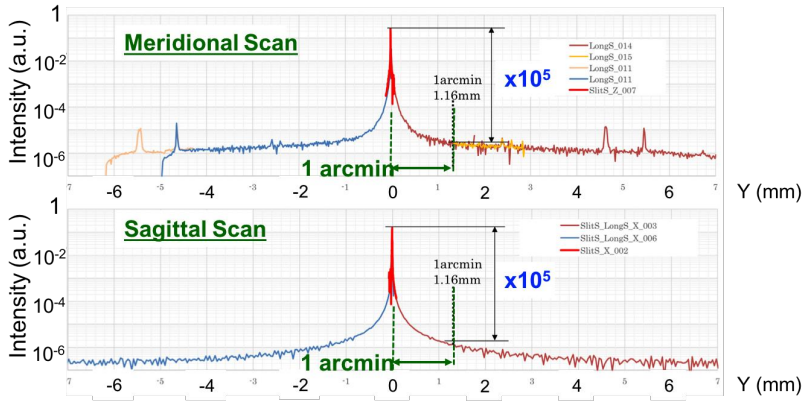

Figure 7. Large-angle scattering profiles of the Engineering Mirror #3, for the meridional (*top*) and the sagittal (*bottom*) directions of the mirror.

Detailed profiles of the focused X-rays at 8 keV with the Engineering Mirror #3 were measured by the wire/knife-edge scans. The entire precision polished mirror area was illuminated with X-rays. Figure 8 shows the intensity profile of the PSF core (left panel) and the integrated energy profile (right panel), in the meridional direction of the mirror. The FWHM of the PSF core profile for the meridional focusing reached at ~0.12 arcsec which is almost identical to the diffraction limit at 8 keV in the meridional direction whose numerical aperture NA ~ 3.2×10^{-5}. The half-power diameter (HPD) of the mirror, as defined by the scanning distance between the position where 25 % of the total 8 keV intensity was detected and that where 75 % was, reached as small as ~0.2 arcsec for the meridional scan. For the sagittal scan, the

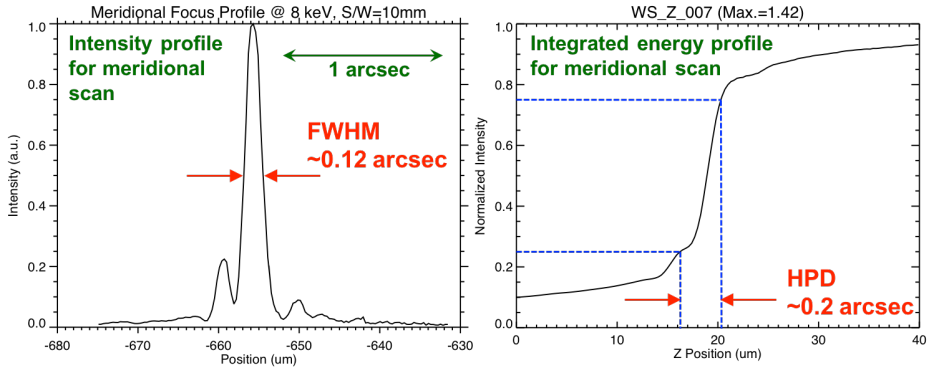

Figure 8. *Left:* Meridional intensity profile of the PSF core of the Engineering Mirror #3, measured with 8 keV X-rays. *Right:* Integrated energy profile in the meridional direction of the mirror.

FWHM of the PSF core profile was ~0.08 arcsec and the HPD ~0.1 arcsec. Due to the large numerical aperture of NA ~ 1.3×10^{-3} for the sagittal direction, the sagittal focusing fell short of the diffraction limit.

The sagittal focal length was measured to be 4016.5−4018.5 mm within the accuracy of the measurement. This is in good agreement with the expected focal length of 4017 mm (designed focal length of the mirror of 4000 mm with the finite X-ray source distance of 950 m taken into account). The meridional focal length was not determined due to the large focus depth associated with the small numerical aperture in the meridional direction. Hence we conclude that the large astigmatism noted in the Engineering Mirror #2 was well corrected in the Engineering Mirror #3, within the accuracy of ~±1 mm.

Table 3 summarizes the X-ray focusing performance of the Engineering Mirror #3.

Table 3. Summary of the X-ray focusing performance at 8 keV of the Engineering Mirror #3.

Item	Description	Note
Focal length		
Sagittal focus	4016.5−4018.5 mm	In agreement with the design value.
Meridional focus	Not determined	Due to the large focus depth.
PSF core profile		
Sagittal focus	FWHM: ~0.08 arcsec, HPD: ~0.1 arcsec	
Meridional focus	FWHM: ~0.12 arcsec [*], HPD: ~0.2 arcsec	[*] Nearly diffraction limited.
Large-angle scattering	$\ll 10^{-3}$ (nearly 10^{-4}) at 10 arcsec off-axis $< 10^{-5}$ at 1 arcmin off-axis	For both sagittal and meridional directions.

5. SUMMARY

Based on the extensive evaluation of the metrology measurements during the precision polish and X-ray measurements of the focusing performance on the Engineering Mirror #2, we have identified areas of improvement for fabricating the next Engineering Mirror #3[17]. Through improvement in the precision polish by adopting a smaller polishing head for the deterministic MRF polish and refined smoothing, as well as the optimized order in combining the deterministic polish and smoothing, we have achieved a precision Wolter surface whose figure error PSD comparable to, or even exceeding in many spatial frequencies, that of the *Chadra* mirror (Figure 3). Furthermore, careful characterization of the mechanical measurement system used during the precision polish revealed the existence of a systematic error which we identified most likely to have caused the large astigmatism found during the X-ray measurements of the Engineering Mirror #2. The precision polish of the Engineering Mirror #3 was performed by correcting this systematic error.

Characterization on the X-ray focusing performance of the Engineering Mirror #3 was carried out in December 2016, at SPring-8 BL29XUL/EH4. By illuminating 8 keV parallel X-rays to the entire precision polish area of the parabola segment, the Engineering Mirror #3 attained sub-arcsecond focusing in terms of HPD (which remained at ~3 arcsec for the Engineering Mirror #2) both in the meridional and the sagittal directions, with the meridional focusing reaching almost the diffraction limit. Although we understand it is not fair to say, due to the large difference in size of the mirror area, the attained focusing performance is even better than that of the *Chandra* mirror hence we think the focusing performance presented here is the best one among Wolter mirrors aiming for X-ray observations from space[20].

Wide-angle scattering of reflected X-rays was comfortably suppressed to a level below 10^{-5} of the on-axis intensity at the 1-arcmin off-axis position for both sagittal and meridional directions. It should be noted that the scattering level was suppressed to a level of nearly 1×10^{-4} of the on-axis intensity even at the 10-arcsec off-axis position. These low-scattering features of the mirror would be particularly powerful when one wants to investigate, by avoiding scattered X-rays from nearby bright features, rather dark regions of the X-ray solar corona where important physical processes are thought to be ongoing during flares. Besides the achievement of the sub-arcsecond/low-scattering focusing performance, the correction of the systematic error in the mechanical measurement system successfully removed the large astigmatism (but corresponded to a sag error of only 6.5 nm for each of the mirror areas) present in the Engineering Mirror #2.

Through the development effort thus far made, we believe that we have established methodology for fabricating, and measuring in X-rays, precision Wolter mirrors to be used for astrophysical observations from space, at least for a mirror size of 32.5 mm ×10 mm (for each of the parabola and hyperbola segments).

While the size of the precision mirror area of the Engineering Mirror #3 is already sufficient for observing bright X-ray features in solar flares (coupled with photon-counting capability for the focal-plane detector), our next step will be to increase the size of the precision mirror to better observe, with good spatial and temporal resolution, rather dark features in the flaring X-ray solar corona. For this purpose, our next step would be to look into the feasibility of precision-polishing on either side of the present precision mirror area of the Engineering Mirror #3 (see Figure 4). Meanwhile, we are seeking for flight opportunities of our sub-arcsecond Wolter mirror(s) with satellite and/or sounding rocket missions.

ACKNOWLEDGEMENT

The X-ray mirror development activities have been supported by Japan Society for the Promotion of Science (JSPS) KAKENHI Grant-in-Aid for Challenging Exploratory Research, JP24654053, and Grant-in-Aid for Scientific Research (A), JP26247031. We are also grateful to the support so far made from the strategic R&D fund for future space missions from ISAS/JAXA Space Sciences Steering Committee.

The fabrication and X-ray measurements of the engineering Wolter mirrors #1, #2, and #3 were supported by numerous people. Dr. Hiroki Nakamori of Osaka University (now also at JTEC Corp.) and Dr. Akihiko Nishihara and Dr. Ryosuke Fukui of Osaka University are deeply acknowledged for participating in and performing X-ray measurements of the mirrors at SPring-8 BL29XUL. We express our sincere gratitude to Dr. Tetsuya Ishikawa, Director of RIKEN Harima Branch, and Ms. Yasuko Matsumoto of SPring-8/RIKEN for their crucial support in administrative aspects for successfully conducting X-ray measurements of the Engineering Mirror #3 at SPring-8, and to Dr. Hirokatsu Yumoto of SPring-8/RIKEN for valuable conversations with him during the X-ray measurements. We deeply acknowledge Messrs. Hirohiko Shinonaga, Akihiko Gomi, Shinya Mochizuki, Kotaro Akutsu, Jun Watanabe, Itaru Otsuka, and Yuichiro Hashimoto of Canon Inc., and Messrs. Takayuki Miyazawa and Eiji Hara of Natsume Optical Corp. for their continuous enthusiasm and participation in the development of precision Wolter mirrors for future X-ray observations of the Sun.

REFERENCES

1. Ogawara, Y., Takano, T., Kato, T., Kosugi, T., Tsuneta, S., Watanabe, T., Kondo, I., and Uchida, Y., "The Solar-A Mission: An Overview," Sol. Phys. 136, 1-16 (1991).
2. Kosugi, T., Matsuzaki, K., Sakao, T., Shimizu, T., Sone, Y., Tachikawa, S., Hashimoto, T., Minesugi, K., Ohnishi, A., Yamada, T., Tsuneta, S., Hara, H., Ichimoto, K., Suematsu, Y., Shimojo, M., Watanabe, T., Shimada, S., Davis, J. M., Hill, L. D., Owens, J. K., Title, A. M., Culhane, J. L., Harra, L. K., Doschek, G. A., and Golub, L., "The *Hinode* (Solar-B) Mission: An Ovewview," Sol. Phys. 243, 3-17 (2007).
3. Tsuneta, S., Takahashi, T., Acton, L. W., Bruner, M. E., Harvey, K. L., and Ogawara, Y., "Global Restructuring of the Coronal Magnetic Fields Observed with the Yohkoh Soft X-Ray Telescope," PASJ 44, L211-L214 (1992).
4. Masuda, S., Kosugi, T., Hara, H., Tsuneta, S., and Ogawara, Y., "A loop-top hard X-ray source in a compact solar flare as evidence for magnetic reconnection," Nature 371, 495-497 (1994).
5. Tsuneta, S., Masuda, S., Kosugi, T., and Sato, J., "Hot and Superhot Plasmas above an Impulsive Flare Loop," Ap. J. 478, 787-798 (1997).
6. Gosling, J. T., "The Solar Flare Myth," JGR-A 98, 18937-18949 (1993).
7. Hara, H., Watanabe, T., Harra, L. K., Culhane, J. L., Young, P. R., Mariska, J. T., and Doschek, G. A., "Coronal Plasma Motions Near Footpoints of Active Region Loops Revealed from Spectroscopic Observations with *Hinode* EIS," Ap. J. Lett. 678, L67-L71 (2008).
8. Klimchuk, J. A., "Key aspects of coronal heating," Phil. Trans. R. Soc. A 373, 20140256, 16pp (2015).
9. Cirtain, J. W., Golub, L., Winebarger, A. R., De Pontieu, B., Kobayashi, K., Moore, R. L., Walsh, R. W., Korreck, K. E., Weber, M., McCauley, P., Title, A., Kuzin, S., and DeForest, C. E., "Energy release in the solar corona from spatially resolved mangetic braids," Nature 493, 501-503 (2013).
10. Wolter, H., "Spiegelsysteme streifenden Einfalls als abbildende Optiken für Röntgenstrahlen," Ann. der Physik 445, 94-114 (1952).

11. Misaki, K., Hidaka, Y., Ishida, M., Shibata, R., Furuzawa, A., Haba, Y., Itoh, K., Mori, H., and Kunieda, H., "X-ray telescope onboard Astro-E. III. Guidelines to performance improvements and optimization of the ray-tracing simulator," Applied Optics 44, 916-940 (2005).
12. Zissa, D. E., "AXAF-I High Resolution Mirror Assembly image model and comparison with x-ray ground-test image," Proc. SPIE 3766, 36-50 (1999).
13. Sakao, T., Narukage, N., Shimojo, M., Tsuneta, S., Suematsu, Y., Miyazaki, S., Imada, S., Nishizuka, N., Watanabe, K., Dotani, T., DeLuca, E. E., and Ishikawa, S., "Photon-counting soft X-ray telescope for the Solar-C mission," Proc. SPIE 8148, 81480C, 13 pp. (2011).
14. Sakao, T., Narukage, N., Imada, S., Suematsu, Y., Shimojo, M., Tsuneta, S., DeLuca, E. E., Watanabe, K., and Ishikawa, S., "The X-ray/EUV telescope for the Solar-C mission: Science and development activities," Proc. SPIE 8443, 84430A, 11 pp. (2012).
15. Sakao, T., Narukage, N., Shimojo, M., Watanabe, K., Suematsu, Y., Imada, S., and Ishikawa, S., "The soft X-ray photon-counting spectroscopic imager for the Sun," Proc. SPIE 8862, 88620T, 12 pp. (2013).
16. Sakao, T., Narukage, N., Suematsu, Y., Watanabe, K., Shimojo, M., Imada, S., Ishikawa, S., and DeLuca, E. E., "The soft x-ray photon-counting telescope for solar observations," Proc. SPIE 9144, 91443D, 8 pp. (2014).
17. Sakao, T., Matsuyama, S., Kime, A., Goto, T., Nishihara, A., Nakamori, H., Yamauchi, K., Kohmura, Y., Miyake, A., Hashizume, H., Maezawa, T., Suematsu, Y., and Narukage, N., "Development of precision Wolter mirrors for future solar x-ray observations," Proc. SPIE 9603, 96030U, 9pp. (2015).
18. Harris, D. C., "History of Magnetorheological Finishing," Proc. SPIE 8016, 80160N, 22pp. (2011).
19. Ishikawa, T., Tamasaku, K., Yabashi, M., Goto, S., Tanaka, Y., Yamazaki, H., Takeshita, K., Kimura, H., Ohashi, H., Matsushita, T., and Ohta, T., "One km beamline at SPring-8," Proc. SPIE 4145, 1-10 (2001).
20. Horiuchi, N., "View From... XOPT 2017: Evolving X-ray science," Nature Photonics 11, 409-410 (2017).